

The dielectric properties and phase transitions of $(1-x)\text{Pb}(\text{Yb}_{1/2}\text{Ta}_{1/2})\text{O}_3-x\text{PbZrO}_3$

H. Kim^{a,*}, T.H. Hwang^b, J.-H. Kim^a, W.K. Choo^a

^aDepartment of Materials Science and Engineering, Korea Advanced Institute of Science and Technology, 373-1 Guseong-dong, Yuseong-gu, Daejeon, 305-701, South Korea

^bTD1 Team, Corporate R&D Center, Samsung SDI Co., Ltd., 428-5, Gongse-ri, Kiheung-eup, Yongin-City, Gyeonggi-Do, 449-902, South Korea

Abstract

The dielectric properties and phase transition behaviors of antiferroelectric-antiferroelectric $(1-x)\text{Pb}(\text{Yb}_{1/2}\text{Ta}_{1/2})\text{O}_3-x\text{PbZrO}_3$ [(1-x)PYT-xPZ] solid solution system ($0.0 \leq x \leq 0.10$) have been studied by X-ray diffraction, permittivity and E-P hysteresis measurement. With increasing the PbZrO_3 amount, the initially split Bragg peaks (400) and (440) begin to merge into single lines. The temperature of the secondary phase transition of (1-x)PYT-xPZ whose character is relaxor-like decreases rapidly rather than that of the first order transition whose character is frequency independent with increasing the PbZrO_3 addition. From the E-P hysteresis loop measurement, the remanent polarizations and the coercive field of the system go to zero as the temperature and Zr^{4+} concentration increase.

© 2003 Elsevier Ltd. All rights reserved.

Keywords: Dielectric properties; Ferroelectric properties; $(1-x)\text{Pb}(\text{Yb}_{1/2}\text{Ta}_{1/2})\text{O}_3-x\text{PbZrO}_3$; Perovskites

1. Introduction

The lead-based complex perovskites with chemical formula $\text{Pb}(\text{B}'_x\text{B}''_{1-x})\text{O}_3$ have attracted much attention due to industrial and academic interest.^{1,2} Their dielectric behavior is dependent on the chemical composition and geometrical distribution of B-site cations in the perovskite lattice.³

$\text{Pb}(\text{Yb}_{1/2}\text{Ta}_{1/2})\text{O}_3$ (PYT) is a compound of highly ordered perovskite structure.^{4,5} PYT has two successive phase transitions; the first is the paraelectric (PE)-antiferroelectric (AFE) transition at 310 °C and the other is the AFE-ferroelectric (FE) at approximately 177 °C.⁴ This transition pattern is very similar to that of the highly ordered $\text{Pb}(\text{Co}_{1/2}\text{W}_{1/2})\text{O}_3$ (PCW) that also undergoes two successive phase transitions (PE-AFE-FE).⁶ Furthermore it is generally accepted that PCW is antiferroelectric at room temperature.⁷ X-ray and transmission

electron microscopy (TEM) studies on highly ordered PCW have revealed evidences of an incommensurate phase.^{8–10} However the present system less studied before than PCW, also $(1-x)\text{Pb}(\text{Yb}_{1/2}\text{Ta}_{1/2})\text{O}_3-x\text{PbZrO}_3$ system has not been reported.

In this work, antiferroelectric-antiferroelectric (1-x)PYT-xPZ solid solution ceramic system ($0.0 \leq x \leq 0.10$) was investigated by X-ray analysis, the dielectric constant study, E-P hysteresis measurement. The effect of PbZrO_3 addition on the successive phase transition was examined in this study.

2. Experiments

Ceramic samples with the chemical formula of $(1-x)\text{Pb}(\text{Yb}_{1/2}\text{Ta}_{1/2})\text{O}_3-x\text{PbZrO}_3$ were prepared using a conventional mixed-oxide method by reacting the stoichiometric proportions (solid state reaction method) of high purity PbO , Yb_2O_3 , Ta_2O_5 and ZrO_2 powders (Kojundo Chemical Lab Co.). The mixtures were ball-milled in acetone, dried, and then calcined at 900 °C for 3 h in an MgO crucible. The calcined pallets were

* Corresponding author. Tel.: +82-42-869-4253; fax: +82-42-869-4273.

E-mail address: heesan@kaist.ac.kr (H. Kim).

reground, pressed and sintered at 1050 °C for 1 h. X-ray diffraction experiments were carried out on a two-circle Rigaku Rotaflex X-ray diffractometer (D/max-RB). Specimens for the dielectric constant and E–P hysteresis loop investigations were electroded with silver paste by firing at 600 °C for 5 min. The dielectric constant was measured at several frequencies between 1 kHz and 1 MHz using a Hewlett Packard 4194A Impedance/Gain Phase Analyzer on the heating cycle at a constant rate of 4 °C/min. E–P hysteresis loops were measured on a Sawyer–Tower hysteresis analyzer at 60 Hz.

3. Results and discussion

3.1. X-ray measurement

It was reported that room temperature $\text{Pb}(\text{Yb}_{1/2}\text{Ta}_{1/2})\text{O}_3$ ($x=0.0$) shows monoclinic distortions from the perovskite crystal structure.⁵ Fig. 1 shows the compositional dependence of X-ray powder diffraction profiles of $(1-x)\text{PYT}-x\text{PZ}$ compounds at room temperature in the PYT-rich region. For pure PYT, the characteristic

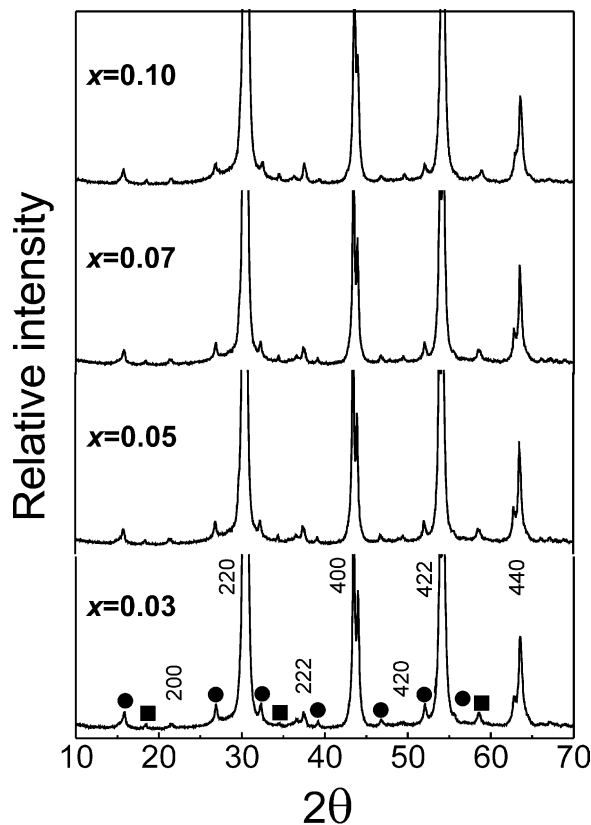


Fig. 1. X-ray diffraction patterns of $(1-x)\text{PYT}-x\text{PZ}$ solid solution at room temperature: ■; reflections due to the B-site (Yb^{3+} , Ta^{5+} , Zr^{4+}) cation ordering, ●; reflections due to antiparallel cation (Pb^{2+}) displacements. The indexing of superlattice lines was done based on the double perovskite cell.

splitting of the (440) lines on X-ray diffraction pattern can be interpreted as arising from orthorhombically distorted ABO_3 type subcells with the pseudo-monoclinic cell.¹¹ The diffraction patterns are composed of two types of superlattice reflection lines. One represents ordering of B-site atoms whose intensity depends on the difference of atomic scattering factor between B-site atoms and the other represents antiparallel Pb cation shift, which are marked solid squares and circles, respectively. This diffraction pattern is almost same as that of $\text{PbYb}_{1/2}\text{Nb}_{1/2}\text{O}_3$.¹² With increasing Zr^{4+}

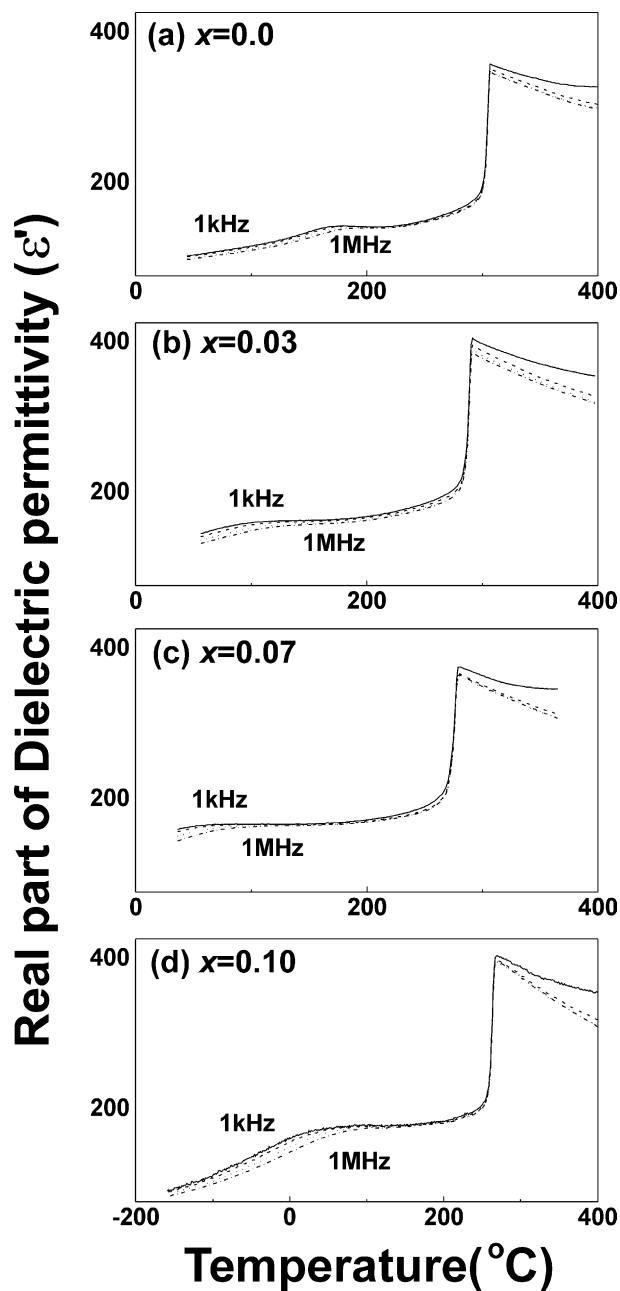


Fig. 2. Temperature dependence of dielectric constant of the $(1-x)\text{PYT}-x\text{PZ}$ system at various frequencies (1 kHz–1 MHz).

substitution, both types of the superlattice reflections are however retained, while the split fundamental lines (400) and (440) gradually merge into single lines. According to the XRD data, the crystal structure does not change macroscopically, but we do not exclude the possibility of change in symmetry from monoclinic to pseudocubic.

3.2. Dielectric constant measurement

Fig. 2 shows the temperature dependence of the dielectric constant ϵ' for the $(1-x)$ PYT– x PZ ceramic system on heating for series of different Zr^{4+} concentrations. Pure PYT shows a frequency independent dielectric behavior at 310° and a frequency dependent one near 177°⁴. With increasing the Zr^{4+} concentration (x), the transition temperature (T_t) of maximum dielectric constant (ϵ'_{max}) decreases ($x=0.0$; $T_t=306$ °C, $x=0.10$; $T_t=268$ °C). The secondary transition is diffuse and characterized by the frequency dependence and the temperature of the transition (T_m) decreases rapidly ($x=0.0$; $T_m=167$ °C at 1 kHz, $x=0.10$; $T_m=33$ °C at 1 kHz) with increasing the Zr^{4+} substitution. In the PYT–PT solid solution with the Ti^{4+} composition, the

broadening of the ϵ' vs. T at the first order phase transition comes from the breaking of the long range order of Yb^{3+} and Ta^{5+} by Ti^{4+} addition.¹¹ However, in this solid solution system, the sharp phase transition is retained with the Zr^{4+} addition.

3.3. E–P hysteresis loop measurement

Pure PYT ($x=0$) has two clearly successive phase transitions.⁴ The primary is PE–AFE at 310 °C and the secondary is AFE–FE phase transition at about 177 °C. We have to determine whether this secondary transition is indeed an AFE–FE transition in $(1-x)$ PYT– x PZ system, and this can be verified by the E–P hysteresis loop measurement. Fig. 3 shows the E–P hysteresis curves of $(1-x)$ PYT– x PZ at $x=0.03$, $x=0.07$ and $x=0.10$ compositions. At each composition, it has a very small remanent polarization ($x=0.03$; $P_r=0.05$ $\mu C/cm^2$) at -45 °C. This is evident that a weak ferroelectric phase exists below the secondary transition temperature. As temperature and Zr^{4+} concentration increase, both the remanent polarization P_r and the coercive field E_c diminish. This means that the anti-ferroelectric phase is gradually stabilized by PZ in conjunction with the disappearance of the secondary dull peak as shown in Fig. 2. Fig. 4 is the XRD patterns of the 0.93PYT–0.07PZ composition with the temperature at -150 , 160 and 350 °C. It does not show any macroscopic crystal structural change at the second transition. On the other hand, the crystal structure of $(1-x)$ PYT– x PZ at the first transition is converted to pseudocubic structure. In conjunction with the Fig. 2(c), Fig. 3(d), (e) and (f), the low temperature phase below the second

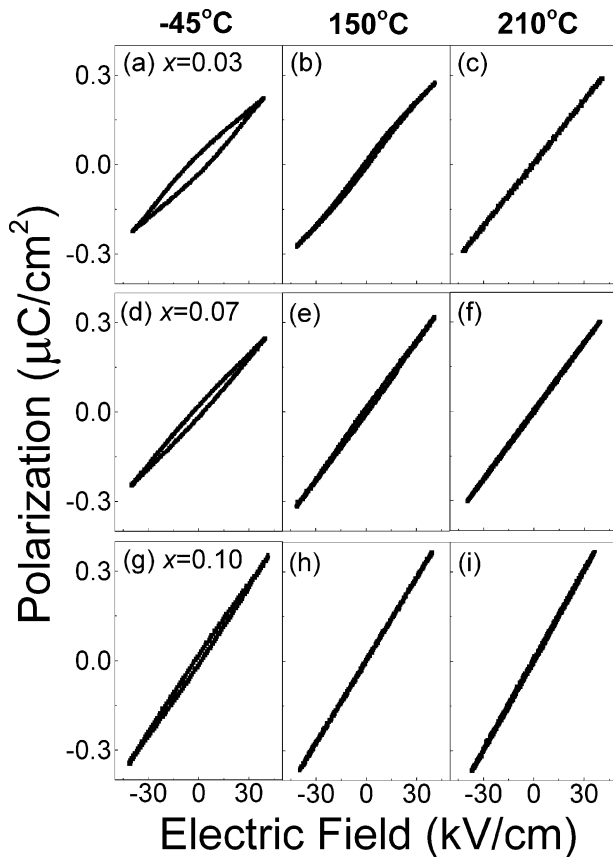


Fig. 3. E–P hysteresis loop of 0.97PYT–0.03PZ: (a), (b), (c), of 0.93PYT–0.07PZ: (d), (e), (f) and of 0.90PYT–0.10PZ: (g), (h), (i) at given temperatures.

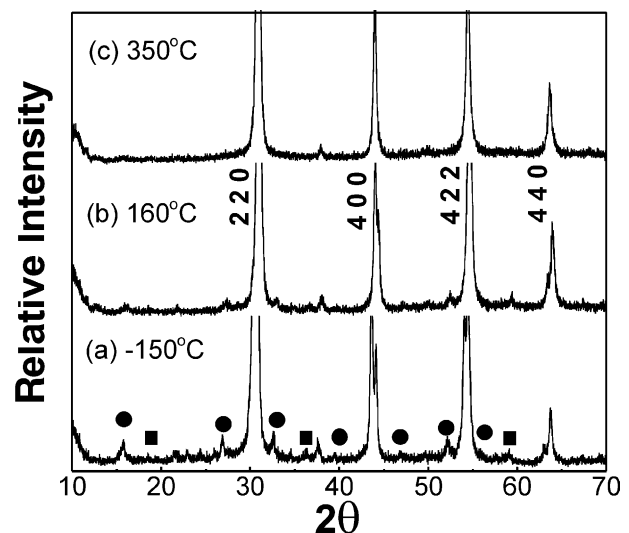


Fig. 4. Temperature dependence of the X-ray diffraction patterns for 0.93PYT–0.07PZ sample: ■; reflections due to the B-site (Yb^{3+} , Ta^{5+} , Zr^{4+}) cation ordering, ● reflections due to antiparallel cation (Pb^{2+}) displacements.

phase transition is an FE with a Pb-ion lattice modulation. Above the second transition temperature, its phase is AFE and goes to PE after the first order phase transition.

4. Conclusions

The crystal structure of $(1-x)\text{Pb}(\text{Yb}_{1/2}\text{Ta}_{1/2})\text{O}_3-x\text{PbZrO}_3$ solid solutions for $0.0 \leq x \leq 0.10$ does not change macroscopically, and remains the monoclinic structure like that of pure PYT. For $x=0.10$, the phase transition behavior is similar to that of pure PYT, but the temperature of the secondary transition inherent to PYT decreases more rapidly than that of the primary transition with increasing the Zr^{4+} concentration. Below the secondary transition temperature of $0.93\text{PYT}-0.07\text{PZ}$, it can be verified that its phase is a FE with small polarization. As temperature increases, its phase becomes PE via AFE. As the Zr^{4+} ion concentration increases further below $x=0.10$, the polarization gradually decreases and finally disappears. It means that AFE becomes predominant. This phenomenon is confirmed by E–P hysteresis measurement.

Acknowledgements

This research was supported by the International Cooperation Research Program of the Ministry of Science & Technology. The authors deeply appreciate this support.

References

1. Burfoot, J. C. and Taylor, G. W., *Polar Dielectrics and Their Applications*. Macmillan, London, 1979.
2. Lines, M. E. and Glass, A. M., *Principles and Applications of Ferroelectrics and Related Materials*. Clarendon, Oxford, 1977.
3. Randall, C. A. and Bhalla, A. S., Nanostructural-property relation in complex lead perovskites. *Jpn. J. Appl. Phys.*, 1990, **29**, 327–333.
4. Yasuda, N. and Konda, J., Successive paraelectric-antiferroelectric phase transitions in highly ordered perovskite lead ytterbium tantalate. *Appl. Phys. Lett.*, 1993, **62**, 535–537.
5. Yasuda, N. and Konda, J., Ferroelectric in highly ordered perovskite lead ytterbium tantalate. *Ferroelectrics*, 1994, **158**, 405–410.
6. Hachiga, T., Fujimoto, S. and Yasuda, N., Pressure and temperature dependence of dielectric properties $\text{Pb}(\text{Co}_{1/2}\text{W}_{1/2})\text{O}_3$. *Jpn. J. Appl. Phys.*, 1985, **24**(3), 239–241.
7. Bonin, M., Paciorek, W., Schenk, K. J. and Chapuis, G., X-ray study of and structural approach to the incommensurate perovskite Pb_2CoWO_6 . *Acta Cryst.*, 1995, **B51**, 48–54.
8. Randall, C. A., Bhalla, A. S., Shrout, T. R. and Cross, L. E., Classification and consequences of complex lead perovskite ferroelectrics with regard to B-site cation order. *J. Mater. Res.*, 1990, **5**, 829–834.
9. Randall, C. A., Markgraf, S. A., Bhalla, A. S. and Baba-Kishi, K., Incommensurate structures in highly ordered complex perovskites $\text{Pb}(\text{Co}_{1/2}\text{W}_{1/2})\text{O}_3$ and $\text{Pb}(\text{Sc}_{1/2}\text{Ta}_{1/2})\text{O}_3$. *Phys. Rev. B*, 1989, **40**, 413–416.
10. Baba-Kishi, K. Z. and Barber, D. J., Transmission electron microscope studies of phase transitions in single crystals and ceramics of ferroelectric $\text{Pb}(\text{Sc}_{1/2}\text{Ta}_{1/2})\text{O}_3$. *J. Appl. Cryst.*, 1990, **23**, 43–54.
11. Park, S. B. and Choo, W. K., Structural and dielectric studies of the phase transitions in $\text{Pb}(\text{Yb}_{1/2}\text{Ta}_{1/2})\text{O}_3\text{-PbTiO}_3$ ceramics. *Jpn. J. Appl. Phys.*, 2000, **39**, 5560–5564.
12. Kwon, J. R. and Choo, W. K., The antiferroelectric crystal structure of the highly ordered complex perovskite $\text{Pb}(\text{Yb}_{1/2}\text{Nb}_{1/2})\text{O}_3$. *J. Phys.: Condens. Matter*, 1991, **3**, 2147–2155.